EXPERIMENTAL SIMULATION OF MANIPULATOR BASE COMPLIANCE

Harry West
Norbert Hootsmans
Steven Dubowsky
Nathan Stelman

Department of Mechanical Engineering
Massachusetts Institute of Technology
Cambridge MA 02139

Abstract

Many future applications of robotic systems will require manipulators to operate from moving vehicles. Such vehicles will be compliant in comparison to the rigid bases on which most manipulators are mounted today. Base compliance can seriously degrade system performance. Statically base compliance may lead to error in the position of the end effector, and dynamically base compliance may interact with the motion of the manipulator and impair the stability of the system. The accuracy of the manipulator may be improved by modelling the base compliance and compensating for its deflection. Further improvement in accuracy may be achieved by endpoint feedback control of the position of the end effector relative to the task frame. A Vehicle Emulator System (VES) has been developed for experimental investigation of the static and dynamic behavior of manipulators mounted on compliant bases. The VES operates under admittance control and can experimentally simulate a wide variety of linear and non-linear six-degree-of-freedom compliances. A series of experiments are described that use modelling of the base compliance and end point control to achieve precise positioning of the end effector of a manipulator manipulator mounted on a compliant base.

1 Introduction

Many future applications of robotic systems will require manipulators to operate from moving vehicles. Such vehicles will be compliant in comparison to the rigid bases on which most manipulators are mounted today. Examples of manipulators on complaint bases are mobile robotic systems for nuclear environments, and *Field Material Handling robots* such as the one shown in Figure 1. An extreme example of a compliant base is a manipulator free floating in space, which is a base compliance with no stiffness or damping.

The compliance at the base of the robot may seriously degrade the performance of the manipulator. Statically the base compliance may lead to error in the position of the end effector, and dynamically the base compliance may interact with the motion of the manipulator and impair the stability of the system. It is possible to improve the accuracy of the manipulator by modelling the base compliance and compensating for the deflection at the end effector. However, it may be difficult to obtain an accurate model of the base compliance. Further improvement in the accuracy of the manipulator can be achieved by directly measuring the position of the end effector relative to the task frame, and controlling the motion of the end effector relative to the task.

Figure 1. Mobile Robot

A *Vehicle Emulator System* has been developed for experimental investigation of the behavior of manipulators mounted on compliant or moving bases. The VES operates under admittance control and can experimentally simulate a wide variety of linear and non-linear six-degree-of-freedom compliances. A description of the VES is given in the Appendix. The goal in developing this apparatus was to provide a general purpose vehicle emulation system with the capabilities to:

(a) Impose an arbitrary trajectory on the base of a manipulator
(b) Emulate the weightlessness of a manipulator free floating in space
(c) Emulate a vehicle suspension including its non-linear characteristics

Experimental work on (a) and (b) has been described in [West, Papadopoulos, Dubowsky and Cheah 1989; Dubowky, Paul and West 1988; Dubowsky and Tanner 1987; Lynch 1987].

This paper describes a series of experiments using the vehicle emulator system to simulate the behavior of a manipulator on a compliant base. The experiments investigate the potential of compliant modelling and end point control to compensate for the error in the position of the end effector caused by base compliance. This work is motivated by the challenge of achieving precise positioning of a large field material handling robot such as the one shown in Figure 1.

2 End Effector Deflection due to Base Compliance

A One Degree of Freedom Example

An analysis of the deflection of the end effector due to compliance at the base will be developed with reference to a simple one-degree-of-freedom example before the more general case is presented. The manipulator shown in Figure 2 has a single joint, about its z_1 axis, and is mounted on a base with compliance about the y-axis, represented by the vehicle emulator system. The reference frame is attached to the center of the force sensor which is also the center of compliance. The compliance has been chosen to be attached to the inertial frame rather than the moving frame, but for the one degree of freedom example this choice has no effect.

The moment at the center of compliance is given by:

$$\underline{\mathbf{m}} = {}^{B}\underline{\mathbf{r}} \times \underline{\mathbf{f}} + \underline{\mathbf{m}}_0 \qquad (1)$$

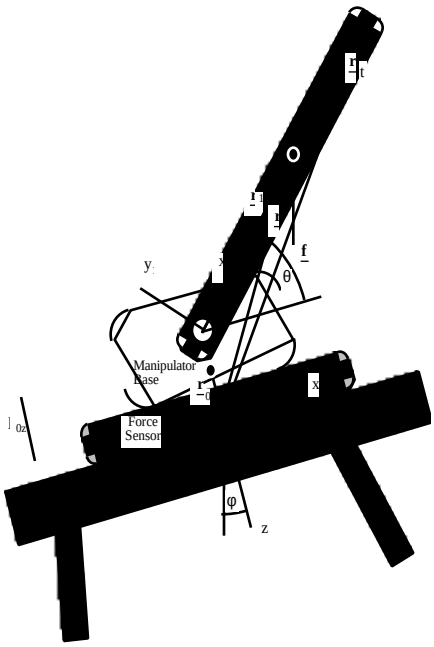

Figure 2. Simple One-Degree-of-Freedom Manipulator Mounted on a Compliant Base

where ${}^{B}\underline{\mathbf{r}}$ is the position of the center of mass of the moving link in the base reference frame, $\underline{\mathbf{f}}$ is the gravitational load on the center of mass of the moving link in the base reference frace, and $\underline{\mathbf{m}}_0$ is the moment due to the weight of the base of the manipulator.

The moment at the base consists of the terms:

$$\underline{\mathbf{m}} = \begin{bmatrix} m_x \\ m_y \\ m_z \\ 1 \end{bmatrix} \tag{2}$$

and the gravitational load on the link is given by the product of the mass and the acceleration due to gravity:

$$\underline{\mathbf{f}} = \begin{bmatrix} -M_1\ g \sin\varphi \\ 0 \\ M_1\ g \cos\varphi \\ 1 \end{bmatrix} \tag{3}$$

where M_1 is the mass of the link and φ is the angle through which the base has complied.

${}^{B}\underline{\mathbf{r}}$, can be described in terms of $\underline{\mathbf{r}}_1$, the position of the center of mass in the link frame, using the transformation matrices $\mathbf{T}_0$ and $\mathbf{T}_1$:

$${}^{B}\underline{\mathbf{r}} = \mathbf{T}_0\ \mathbf{T}_1\ \underline{\mathbf{r}}_1 \tag{4}$$

where $\mathbf{T}_0$ is given by:

$$\mathbf{T}_0 = \begin{bmatrix} 1 & 0 & 0 & l_{0x} \\ 0 & 0 & 1 & l_{0y} \\ 0 & -1 & 0 & -l_{0z} \\ 0 & 0 & 0 & 1 \end{bmatrix} \tag{5}$$

and $\mathbf{T}_1$ is given by:

$$\mathbf{T}_1 = \begin{bmatrix} C_1 & -S_1 & 0 & 0 \\ S_1 & C_1 & 0 & 0 \\ 0 & 0 & 1 & 0 \\ 0 & 0 & 0 & 1 \end{bmatrix} \tag{6}$$

where C_1 is an abreviation for cosine(θ) and S_1 for sine(θ). The vector $\underline{\mathbf{r}}_1$ consists of:

$$\underline{\mathbf{r}}_1 = \begin{bmatrix} r_{1x} \\ r_{1y} \\ r_{1z} \\ 1 \end{bmatrix} \tag{7}$$

Note that that the systems of frames shown in Figure 2 differ from the standard Denavit-Hartenberg notation; frame i is attached at joint i rather than at joint i+1. This notation is used to simplify the analysis.

The resulting moment at the base of the manipulator is:

$$\begin{bmatrix} m_x \\ m_y \\ m_z \\ 1 \end{bmatrix} = \underline{\mathbf{m}}_0 + \begin{bmatrix} (r_{1z}+l_{0y})\, M_1 g\cos\varphi \\ (l_{0z} + S_1 r_{1x} + C_1 r_{1y})\, M_1 g\sin\varphi - (l_{0x} + C_1 r_{1x} - S_1 r_{1y})\, M_1 g\cos\varphi \\ (l_{0y} + r_{1z})\, M_1 g\sin\varphi \\ 1 \end{bmatrix} \tag{8}$$

where $\underline{\mathbf{m}}_0$ is the moment of the tilted base and is given by:

$$\underline{\mathbf{m}}_0 = \begin{bmatrix} r_{0y}\, M_0\, g\cos\varphi \\ r_{0z}\, M_0\, g\sin\varphi - r_{0x}\, M_0\, g\cos\varphi \\ r_{0y}\, M_0\, g\sin\varphi \end{bmatrix} \tag{9}$$

and $\underline{\mathbf{r}}_0$ is the location of the center of mass of the base relative to the force sensor frame.

The moments about the y-axis are a function of the position of the manipulator:

$$m_y = [r_{0z} M_0 + (l_{0z} + S_1 r_{1x} + C_1 r_{1y}) M_1]\, g\sin\varphi - [(l_{0x} + C_1 r_{1x} - S_1 r_{1y}) M_1 + r_{0x} M_0]\, g\cos\varphi \tag{10}$$

which can be written in the form

$$m_y = A\sin\varphi + B\cos\varphi \tag{11}$$

However, the base deflection angle, φ, is a function of the base compliance:

$$\varphi = m_y / K_y \tag{12}$$

where K_y is the base stiffness about the y-axis. The base deflection angle can be solved for iteratively.

For relatively stiff bases the angle of deflection will be small and a small angle approximation can be used:

$$K_y \varphi = A \varphi + B \tag{13}$$

in which case:

$$\varphi = \frac{B}{K_y - A} \tag{14}$$

Using this equation, as $A \rightarrow K_y$ then $\varphi \rightarrow \infty$, that is to say if the moment due to the out of balance mass increases with φ at a faster rate than the restoring moment due to the stiffness of the base, then the system is unstable and may "collapse under its own weight". It can be shown that for $K_y \geq A$ the base will reach a position of stable equilibrium.

The deflected position of the end effector due to base compliance is given by:

$$\underline{\mathbf{x}}_t = \mathbf{R}_\varphi \underline{\mathbf{r}}_t \tag{15}$$

where $\underline{\mathbf{r}}_t$ is the (4 × 1) vector from the center of compliance to the end effector in the base frame, and $\mathbf{R}_\varphi$ is the rotation matrix for an angle φ about the y-axis:

$$\mathbf{R}_\varphi = \begin{bmatrix} C_\varphi & 0 & S_\varphi & 0 \\ 0 & 1 & 0 & 0 \\ -S_\varphi & 0 & C_\varphi & 0 \\ 0 & 0 & 0 & 1 \end{bmatrix} \tag{16}$$

An approximation to the appropriate end effector correction for the base compliance is $-\Delta \mathbf{x}_t$, however, since φ is itself a function of the position of the links of the manipulator, the correction must be made iteratively.

B. Extension to the General Case

The method described in the previous section can be generalized for multi-degree of freedom manipulators mounted on a base with six degrees of freedom of compliance.

The force and moment vector with respect to the base frame is given by:

$$\begin{bmatrix} \underline{\mathbf{f}} \\ \underline{\mathbf{m}} \end{bmatrix} = \begin{bmatrix} M_t \, \underline{\mathbf{g}} \\ M_t \, \underline{\mathbf{r}} \times \underline{\mathbf{g}} \end{bmatrix} = \begin{bmatrix} M_t \, \underline{\mathbf{g}} \, \underline{\mathbf{v}} \\ M_t \, g \, \mathbf{V} \, \underline{\mathbf{r}} \end{bmatrix} \tag{17}$$

where M_t is the total mass of the manipulator, $\underline{\mathbf{g}}$ is the acceleration of gravity, $\underline{\mathbf{r}}$ is the position vector of the manipulator center of mass with respect to the base frame, $\underline{\mathbf{v}}$ is a vector whose elements v_i are the components of the unit vector parallel to $\underline{\mathbf{g}}$ in the base frame and $\mathbf{V}$ is the corresponding matrix whose elements V_i are the components of the unit vector parallel to $\underline{\mathbf{g}}$ in the base frame.

$$M_t = M_0 + M_1 + \ldots . \; M_n \tag{18}$$

where M_i are the masses of the links of the manipulator.

$$\underline{\mathbf{r}} = \begin{bmatrix} r_x \\ r_y \\ r_z \end{bmatrix} \tag{19}$$

$$\underline{\mathbf{v}} = \begin{bmatrix} f_x \\ f_y \\ f_z \end{bmatrix} \tag{20}$$

and,

$$\mathbf{V} = \begin{bmatrix} 0 & f_z & -f_y \\ -f_z & 0 & f_x \\ f_y & -f_x & 0 \end{bmatrix} \tag{21}$$

$M_t g$ represents the weight of the manipulator, and $\mathbf{v}$ and $\mathbf{V}$ are functions of the orientation (direction) cosines of the base.

The position vector of the center of mass of the whole manipulator, $\underline{\mathbf{r}}$, can be calculated as:

$$\underline{\mathbf{r}} = \frac{1}{M_t} \mathbf{T_L} \left(\sum_{i=0}^{n} M_i \mathbf{T}_i \underline{\mathbf{r}}_i \right) \tag{22}$$

where $\underline{\mathbf{r}}_i$ is the position of the center of mass of link i with respect to frame i:

$$\underline{\mathbf{r}}_i = \begin{bmatrix} r_{ix} \\ r_{iy} \\ r_{iz} \\ 1 \end{bmatrix} \quad (i = 0,1,...n) \tag{23}$$

$\mathbf{T}_i$ is the matrix that transforms a postition vector in frame i to a position vector in the base frame, and:

$$\mathbf{T_L} = \begin{bmatrix} 1 & 0 & 0 & 0 \\ 0 & 1 & 0 & 0 \\ 0 & 0 & 1 & 0 \end{bmatrix} \tag{24}$$

$\mathbf{T_L}$ is a 3x4 matrix that removes the last element from the 4x1 vectors in the summation.

For a linear compliance, represented by the (6 × 6) compliance matrix, $\mathbf{C}$, the deflection at the base is given by:

$$\Phi = \mathbf{C} \begin{bmatrix} \underline{\mathbf{f}} \\ \underline{\mathbf{m}} \end{bmatrix} \tag{25}$$

where:

$$\Phi = \begin{bmatrix} \delta_x \\ \delta_y \\ \delta_z \\ \varphi_x \\ \varphi_y \\ \varphi_z \end{bmatrix} \tag{26}$$

however, since both $\underline{\mathbf{f}}$ and $\underline{\mathbf{m}}$ are themselves functions of Φ this expression must be solved

iteratively.

For small base compliance the deflection at the end effector is given by:

$$\Delta \mathbf{x}_t = \mathbf{R}_\varphi' \, \underline{\mathbf{r}}_t \tag{27}$$

where $\Delta \mathbf{x}_t$ is the (6 × 1) vector:

$$\Delta \mathbf{x}_t = \begin{bmatrix} \delta_x \\ \delta_y \\ \delta_z \\ \delta\theta_x \\ \delta\theta_y \\ \delta\theta_z \end{bmatrix} \tag{28}$$

and $\mathbf{R}_\varphi'$ is now given by:

$$\mathbf{R}_\varphi' = \begin{bmatrix} 0 & -\varphi_z & \varphi_y & \delta_x \\ \varphi_z & 0 & -\varphi_x & \delta_y \\ -\varphi_y & \varphi_x & 0 & \delta_z \\ 0 & 0 & 0 & \varphi_x \\ 0 & 0 & 0 & \varphi_y \\ 0 & 0 & 0 & \varphi_z \end{bmatrix} \tag{29}$$

Again an approximation to the appropriate end effector correction for the base compliance is $-\Delta \mathbf{x}_t$, however, since φ is a function of the position of the links of the manipulator the correction must be made iteratively.

3 End Point Control of a Manipulator on a Compliant Base: Experimental Evaluation

By making use of equation (27) it is possible to improve the accuracy of the manipulator by modelling the base compliance and compensating for the deflection at the end effector. However, for most compliant bases that are likely to be encountered in practice the compliance will be difficult to measure, non-linear, and time-varying. Inaccuracies in the estimates of the mass properties of the manipulator or of the load at the end effector will also reduce the usefulness of model-based compensation for obtaining precise positioning at the end effector.

Further improvement in the accuracy of the manipulator can be achieved by directly measuring the position of the end effector relative to the task frame, and controlling the motion of the end effector relative to the task. However, the conditions for stability of a manipulator on a compliant base under endpoint control are not clear. For simplistic models of simple manipulators on a linear compliant base, stability using PD control of the end point can be readily verified [Fasse 1987]. But for real manipulators and real suspensions with non-linear parameters that are difficult both to identify and to model, the conditions for stability are not known. Nonlinear computer simulations can be run using programs such as *Simnon* to verify

particular control schemes, but they are only as accurate as the model they simulate and cannot provide general results.

Rather than invest research effort in developing a complex non-linear computer simulation, simple linear models in the literature were investigated to gain insight into the behavior of idealized systems, and the real robot on a complaint base was simulated *experimentally* using the MIT Vehicle Emulation System. By simulating experimentally we could be sure that none of the non-linear terms had been neglected, and that our model was complete. An industrial manipulator was controlled on a linear compliant base using end point feedback, providing an existence proof for this possibility.

The experimental setup is sketched in Figure 3. A six degree of freedom manipulator, PUMA 250, is mounted on the Vehicle Emulator System. The VES admittance model is programmed to give the desired base compliance matrix. The manipulator makes simple one degree of freedom moves at the shoulder resulting in a change of the moment and force at the base. The static mass properties of the manipulator have previously been measured [West, Papadopoulos, Dubowsky and Cheah 1989] and can be used to give an estimate of the base rotation, φ, and the resulting deflection at the end effector, $\Delta \underline{x}_t$. Applying this end effector correction brings the manipulator to approximately the desired position. More precise positioning is achieved by endpoint control.

The endpoint position feedback sensor is a photodiode measurement of the relative location of the end effector to a referencing laser beam. The photodiode can provide two axis measurement, but in this implementation only the height of the end effector was controlled. The output of the diode amplifier is a voltage proportional to the height of the center of the light spot. The signal from the photodiode is continuous and linear, better than 0.5% linearity at the center of the diode, so the sampling rate is limited only by the cycle time of the control program. The endpont controller regulated the position of the shoulder axis of the manipulator to maintain the position of the laser spot at the center of the photdiode. A PID controller was used to eliminate steady state error. The controller modified the set point of the manipulator controller with a cycle time of 30 ms.

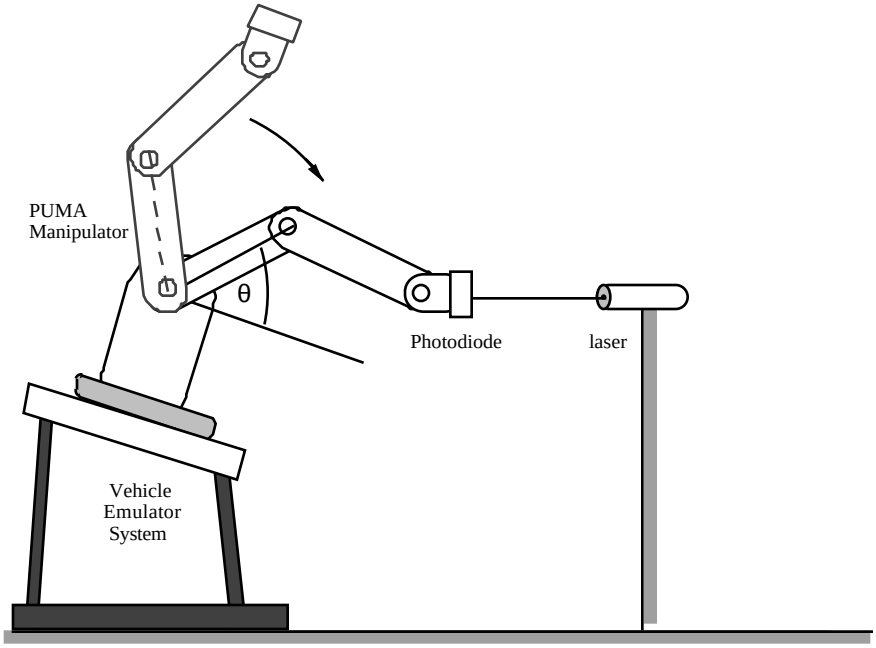

Figure 3. Sketch of Manipulator under Endpoint Feedback Control on a Compliant Base

3 Experimental Results

Three experiments are documented in the graphs below.

A. VES Stationary

Endpoint controller: Kp = 0.3, Kv = 0.0, Ki = 0.036

Initial E. E. position error 9 mm

Under end point control manipulator is able to correct its position error with a rise time of less than 1/30th of a second, and then reduce steady state error down to the sensor noise level within 0.5 seconds with essentially no overshoot, Figure 4.

Figure 4. Endpoint Servoing of Manipulator on Rigid Base

B. VES Compliant: $I = 18\ Kgm^2$, $B = 34\ Nm/rad\ s^{-1}$, $K = 215\ Nm/rad$,

$\zeta = 0.3$, $\omega_n = 0.6$ Hz

Endpoint controller: Kp = 0.3, Kv = 0.0, Ki = 0.036

Initial E. E. position error 17.5 mm

With base compliance the rise time of the endpoint controller is slower and the response more oscillatory, Figure 5. The manipulator is able to correct its position error with a rise time of approximately 1/10th of a second, and then reduce steady state error down to the sensor noise level within 2.0 seconds. The impaired performance may be partly an artifact of the apparatus, for example vibration of the Vehicle Emulator System may be adding a significant amount of noise to the postion and force measurements. Examination of the base torque and angle show that the base compliance contributes to the overshoot of the endpoint controller. The spike on the moment plot clearly indicates the time at which end point control was initiated.

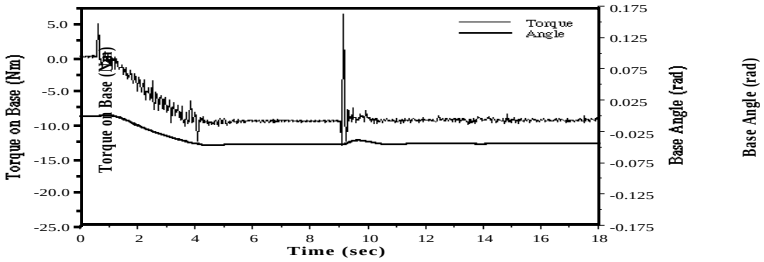

Figure 5. Endpoint Servoing of Manipulator on A Stiff Compliant Base

(a) Base Torque and Angle as the Manipulator Moves

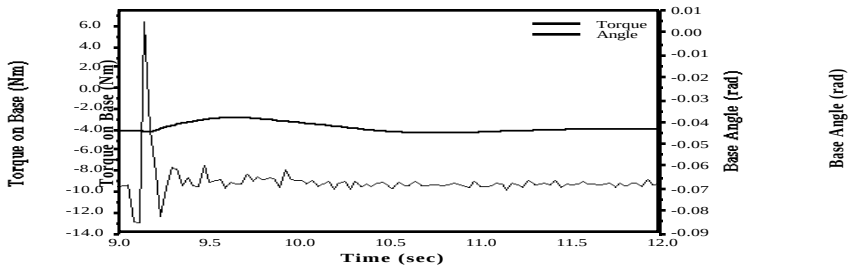

Figure 5. Endpoint Servoing of Manipulator on A Stiff Compliant Base
(b) Detail of Base Torque and Angle

Figure 5. Endpoint Servoing of Manipulator on A Stiff Compliant Base
(c) End Point Position Error Under End Point Control

C. VES Compliant: $I = 10\ Kgm^2$, $B = 23$ Nm/rad s^{-1}, $K = 100$ Nm/rad,
$\zeta = 0.36$, $\omega_h = 0.5$ Hz
Endpoint controller: $Kp = 0.3$, $Kv = 0.0$, $Ki = 0.036$
Initial E. E. position error 57mm

Reducing the stiffness of the base makes the interaction between the motion of the manipulator and the motion of the base more apparent, Figure 6. On a soft compliant base the end point feedback sensor is out of range. The manipulator makes an initial correction using a model of its base compliance to bring the end point sensor into range, and then uses end point control as before. The response is slower and more oscillatory, as would be expected.

The initial correction was made using a model of the base compliance and estimates of the mass properties of the manipulator. The mass properties were measured using the method described in [West, Papadopoulos, Dubowsky, and Cheah 1989]. The parameters identified were:

$p1 = M_1 r_{1x}$ = +0.518 Kg m

$p2 = M_1 r_{1y}$ = +0.309 Kg m

$p3 = M_0 r_{0x} + M_1 l_0$ = -0.006 Kg m

$p4 = M_0 r_{0y} + M_1 (l_{0y} + r_{1z})$ = +0.831 Kg m

$p5 = M_0 r_{0z} + M_1 l_{0z}$ = +3.883 Kg m

These values were substituted into equation (10), and then equation (12) was used to iterate for the expected base moment and deflection. For the initial arm position described by $\theta1=-90^o$, $\theta2=-28^o$, $\theta3=-124^o$, the base moment was measured to be 3.1 Nm. After the arm was moved to a new position described by $\theta1=-90^o$, $\theta2=62^o$, $\theta3=-124^o$, and with a base compliance of 100 Nm/rad, the change in the base moment, m_y, was calculated to be -10.5 ± 0.2 Nm. Adding the initial value, the base moment corresponding to the new arm position was predicted to be -13.6 ± 0.2 Nm. The actual value of the base moment was measured to be -13.5 ± 0.2 Nm, and the corresponding final value of the base angle was measured to be -0.135 radians. Using equation (27) a new arm position was calculated to compensate for the base compliance, bringing the end point sensor into range.

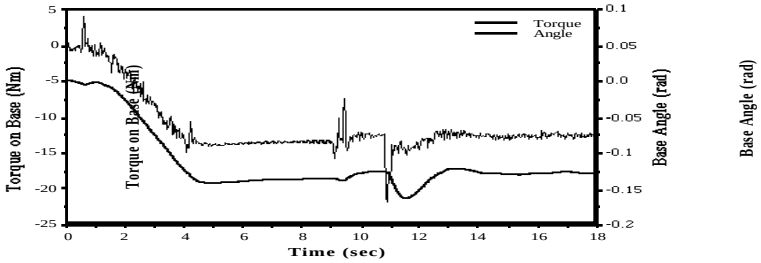

Figure 6. Endpoint Servoing of Manipulator on A Soft Compliant Base

(a) Base Torque and Angle as the Manipulator Moves

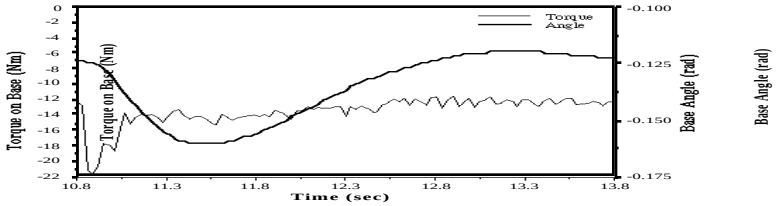

Figure 6. Endpoint Servoing of Manipulator on A Soft Compliant Base

(b) Detail of Base Torque and Angle

Figure 6. Endpoint Servoing of Manipulator on A Soft Compliant Base

(c) End Point Position Error Under End Point Control

4 Conclusions

In the future, robotic manipulators will be increasingly used in applications in which they are not fixed to the factory floor, but are mobile or are mounted on vehicles. Mobile manipulators will be characterized by compliant rather than rigid bases, and such compliance will impair the performance of the manipulator. Statically the base compliance may lead to error in the position of the end effector, and dynamically the base compliance may interact with the motion of the manipulator and cause instability.

A procedure has been developed for calculating the static deflection at the end effector of a manipulator mounted on a compliant base by modelling the compliance characteristics of the base and the mass properties of the manipulator. Using this model, the position of the end effector can be corrected to compensate for the deflection of the base. More accurate positioning of the manipulator can then be achieved using end point feedback control.

The stability conditions for a manipulator on a compliant base under endpoint control are not clear. Rather than develop a complex non-linear computer simulation to investigate this issue, a real robot on a complaint base was simulated *experimentally* using the MIT Vehicle Emulation System. The robot was found to be stable under end point control for a wide range of linear

base compliances.

The Vehicle Emulator System has been built to emulate base compliance. The VES operates under admittance control and can experimentally simulate a wide variety of linear and non-linear six-degree-of-freedom compliances, including terrestrial vehicle compliance and free floating conditions in space. The VES is being used to experimentally evaluate sensors and algorithms for the control of mobile manipulator.

Future work will investigate the stability conditions and performance limits for end point control of manipulators on compliant bases; and will develop algorithms, sensors and other hardware for their control.

Acknowledgements

The support of this work by NASA (Langley Research Center Automation Branch) and the DARPA (US Army Human Engineering Laboratory and the Oak Ridge National Laboratory as agents) is acknowledged. A number of MIT students have made significant contributions to this work; they are Charles Graves, Vijay Krish, Naveed Ismail, and Evangelos Papadopoulos.

References

Dubowsky, S., I. Paul, and H. West, "An Analytical and Experimental Program to Develop Control Algorithms for Mobile Manipulators", Proc. RoManSy '88, Udine, Italy, 1988.

Dubowsky, S. and A. B. Tanner, "A Study of the Dynamics and Control of Mobile Manipulators Subjected to Vehicle Disturbances," Proc IV Int Symp of Robotics Research, Santa Cruz, CA, 1987.

Fasse, E. D., Stability robustness of impedance controlled manipulators coupled to passive environments, S. M. thesis Dept. of Mech. Eng., MIT 1987.

Fresko, M., The Design and Implementation of a Computer Controlled Platform With Variable Admittance, M.S. Thesis, Dept. of Mech. Eng. MIT, Cambridge, MA January, l986.

Lynch, R., Analysis of the Dynamics and Control of a Two Degree of Freedom Robotic Manipulator Mounted on a Moving Base, S. M. Thesis, Dept. of Mech. Eng., MIT, Cambridge, MA 1985.

National Academy, Application of Robotics to Reduce Risk and Improve Effectiveness: A Study for the United States Army, Published by the National Academy Press, Washington, D.C. 1983

Stelman, N., Design and Control of a Six-Degree-of-Freedom Platform with Variable Admittance, S.M. Thesis, Dept. of Mech. Eng., MIT, Cambridge, MA.

West, H., E. Papadopoulos, S. Dubowsky, H. Cheah, "A Method for Estimating the Mass Properties of a Manipulator by Measuring the Reaction Moments at its Base," IEEE Conference on Robotics and Automation, Scottsdale, AZ, 1989.

Appendix - The Vehicle Emulation System

The Vehicle Emulation System consists of a manipulator mounted on an emulator system [Fresko 1986, Stelman 1988]. The experimental manipulator is a six degree of freedom PUMA 250 with a custom joint controller, and the emulator system comprises a six degree of freedom Stewart mechanism, six degree of freedom force sensor, and computer controller. The experimental manipulator and the emulator system are controlled by individual DEC PDP-11/73's, and can be coordinated using a communication link between the two computers. A sketch of the system is shown in Figure A1.

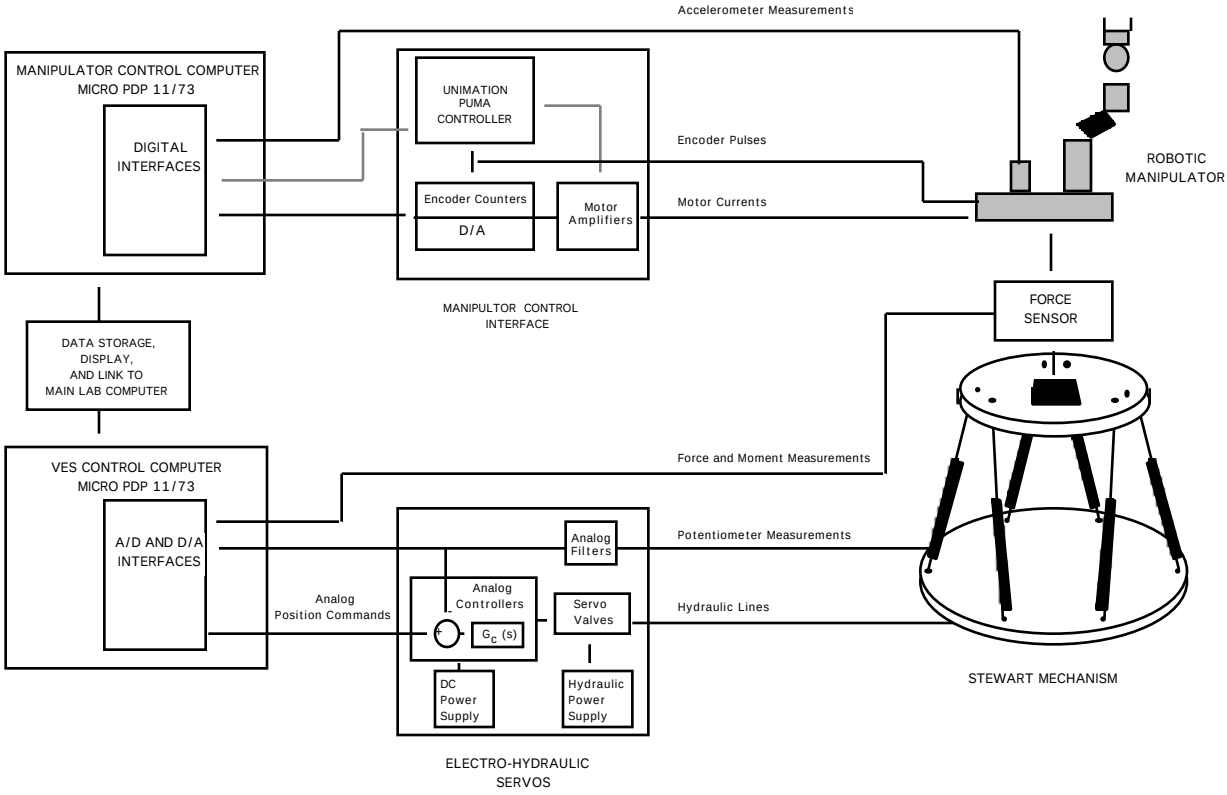

Figure A1. Overview of Space Vehicle Emulation System

The Stewart mechanism and force sensor can, respectively, move and measure forces in any of the three translational directions (x,y,z), and any of the the three rotational directions, ($\theta_x, \theta_y, \theta_z$) possible in general three dimensional space. The platform stands approximately 3 feet of the ground in its home position. The major hardware elements of the Space Vehicle Emulation System are shown in Figure A2, and a photograph of the System is shown in Figure A3.

Figure A2. Mechanical Hardware Elements
of Vehicle Emulation System

Figure A3. Photograph of Vehicle Emulation System

A micro-PDP11/73 is used for trajectory calculation, and also to provide position commands to the analog joint controllers of the Stewart mechanism. The microcomputer is also used to subtract the calculated gravitational load of the manipulator from the force measured by the force sensor for simulating weightless conditions. In addition to trajectory calculation and control, the computer performs a supervisory function checking for approaching violations of the kinematic constraints, and verifies that the joints are following the desired trajectory within allowed error bounds.

The Vehicle Emulator System may be operated in either position driven or admittance control modes. In the position driven mode the VES imposes an arbitrary motion onto the base of the experimental manipulator corresponding, for example, to the motion of a vehicle moving over rough ground. In the admittance control mode, dynamic forces due to manipulator motions are measured by the force sensor and cause the platform to move as if, for example, the manipulator were mounted on a truck suspension or free floating in space.

The admittance control method can be used to simulate vehicles with any dynamic model of the general form:

$$\underline{\mathbf{x}}'' = \underline{\mathbf{f}}\,(\underline{\mathbf{x}}, \underline{\mathbf{x}}', t) \qquad \text{(A1)}$$

where $\underline{\mathbf{x}}$ is the position of the vehicle. The structure of the admittance control mode is shown in Figure A4. The output of the admittance model is the acceleration of the base corresponding to the measured force. The base acceleration is integrated twice to give the desired position trajectory of the compliant base, and then an inverse kinematic model is used to calculate the corresponding leg lengths of the Stewart mechanism. The desired leg lengths are updated each program cycle (every 30 ms for these experiments), and the actual leg lengths are regulated about this series of set points. Under admittance control the Vehicle Emulator System is able to simulate a wide range of different vehicles, for example a robot mounted on a truck with a soft suspension and stabilizing outriggers.

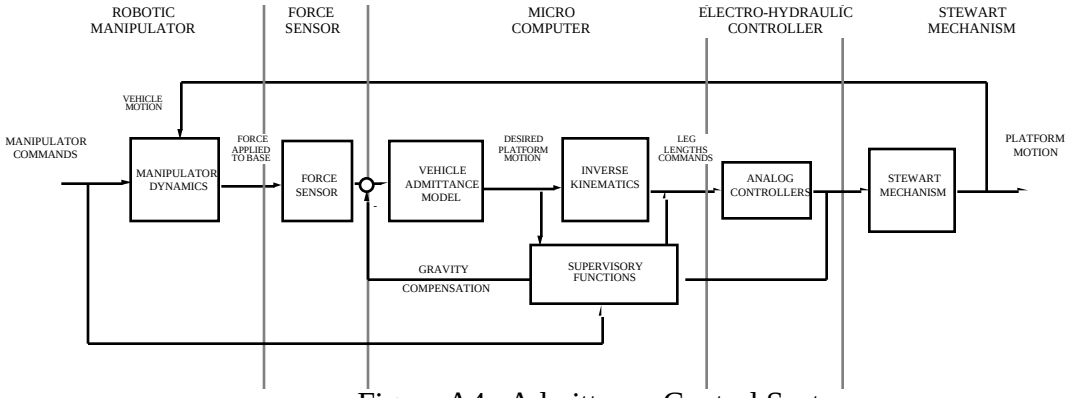

Figure A4. Admittance Control System

The VES is able to simulate vehicle motions of approximately ±150 mm and ±30 degrees in any direction, and currently has a bandwidth of 5 Hz with a 20 kg load. The performance of the vehicle emulator system in its emulation mode is illustrated in Figure A5, which shows the system response to a step change of 45.0 N in vertical load on the platform. The model used by the emulator was for a vehicle whose suspension consisted of a combination of springs and dampers. The model of the vehicle's behavior in the vertical direction is that of a linear second order system, and is shown in the Figure along with the experimentally measured emulator response. The vehicle is modeled for this example as a mass of 175 kg supported by a suspension with a stiffness of 7000 N/m and with a damping constant of 525 N/ms-1, and should respond with a damped oscillation with a natural frequency of 1 Hz and a damping ratio of 0.25. Figure A5 shows that using simple PD control the VES was able to emulate vehicle motion with good accuracy.

Figure A5. Ideal and Measured VES Response

The force sensor measures the sum of the dynamic reaction forces and the gravitational reaction forces. As the position of the links and the orientation of the base of the manipulator change, the gravitational load also changes. For emulating space conditions this load must be subtracted from the load measured by the force sensor to give the dynamic reaction force at the base. The gravitational load of the manipulator on the force sensor can be calculated from the position of the links of the manipulator and the orientation of the base of the manipulator to the vertical, which are known, and the mass properties of the manipulator [West, Papadopoulos, Dubowsky, Cheah 1989].